
Article:
Mahajan, A., Reaney, I.M. orcid.org/0000-0003-3893-6544 and Vilarinho, P.M. (2017) Tuning dielectric properties in ceramics with anisotropic grain structure: The effect of sintering temperature on BaLa4Ti4O15. Materials & Design, 113. pp. 377-383. ISSN 0261-3069

https://doi.org/10.1016/j.matdes.2016.10.040

(revised version of JMAD-D-16-03151R1 to be submitted to Materials & Design, October 2016)

Tuning dielectric properties in ceramics with anisotropic grain structure: the effect of sintering temperature on $BaLa_4Ti_4O_{15}$

Amit Mahajan[1,2], Ian M. Reaney[3] and Paula M. Vilarinho[1*]

[1]Department of Materials and Ceramic Engineering, CICECO – Aveiro Materials Institute, University of Aveiro, 3810-193 Aveiro, Portugal

[2]School of Engineering and Material Science, Queen Mary University of London, London, E1 4NS, UK

[3]Department of Engineering Materials, University of Sheffield, Sheffield, S1 3JD, UK

* corresponding author: paula.vilarinho@ua.pt

Abstract

The orientation and grain aspect ratio, size and distribution of $BaLa_4Ti_4O_{15}$ (BLT) ceramics have been studied as a function of sintering temperature with a view to elucidating a general principle by which the microwave properties (MW) can be understood / tuned in systems which exhibit anisotropic grain structures. For BLT sintered at 1500 ºC, ε_r reaches a maximum of 51, with tan δ minimum at 0.002 and τ_{ε_r} = -17 ppm/ºC but ε_r subsequently varies non-linearly as sintering temperature increases. Since ε_r and $\tau_{\varepsilon_r}$are directly proportional in the absence of a phase transition, the variation of τ_{ε_r} as a function of the sintering temperature is also nonlinear. This behaviour is related with variations in the orientation and grain aspect ratio, size and distribution with the sintering temperature and it is demonstrated that by controlling sintering conditions, microwave dielectric properties can be tuned. It is proposed that this is a general phenomenon which can also be used to explain the variation and tune the properties of other ceramic systems with anisotropic grain structures.

Key words: Microwave materials, dielectrics, $BaLa_4Ti_4O_{15}$, anisotropy, RAMAN, sintering

I. Introduction

The exponential growth of telecommunication systems in the last decade has resulted in demand for new ceramics for microwave (MW) applications. MW ceramics should possess high relative permittivity (ε_r> 20), high quality factor (Q.f > 20,000 GHz) and near zero temperature coefficient of the resonant frequency (τ_f). MW ceramics with high ε_r contribute to the miniaturization of devices, which include COG multilayer capacitors (thick films) and dielectric resonators, antennas and filters (bulk) [1-5]. Materials with ε_r> 40 and $\tau_f$close to zero, such as $CaTiO_3$ - $NdAlO_3$ (CTNA), $ZrTiO_4$ - $ZnNbO_6$ (ZTZN), $BaLa_4Ti_4O_{15}$ (BLT) and $BaNd_2Ti_5O_{14}$ (BNT) [6-11], have potential to be used as resonators or dielectric substrates for antennas either as bulk ceramics or thick films [12]. BLT is a single-phase compound with hexagonal perovskite structure. Detailed and comprehensive research on the crystal structure of BLT have been carried by using X-Ray diffraction, TEM and neutron powder diffraction [13-15]. Moreover, Zheng et al. [6] investigated the structure and microstructure of BLT ceramics by energy-dispersive X-Ray analysis and Raman spectroscopy, concluding that there is a heterogeneous distribution of cations which induces asymmetry in some XRD peaks due to the presence of two hexagonal phases of slightly different composition and lattice parameter. Effectively, bulk ceramics sintered in ambient pressure under the conditions employed by Zheng et al. [6] were composed of two immiscible compositions with differing Ba : La : Ti ratios.

BLT has a large difference between the a (5.5720 Å) and c (22.500 Å) axes and as a result forms plate-like particles [13] during calcination and plate-like grains during sintering. The anisotropy of the crystal structure and particulates is also reflected in its electrical properties. Zheng et al. [6] reported that the relative permittivity of BLT ceramics is 20 % higher perpendicular (ε_r~ 52) to rather than parallel with (ε_r ~ 42) the pressing direction, an effect attributed to alignment of the anisotropic powder particles during pressing. Fukami et al. [16] by using BLT templates (plate-like), maximised the anisotropic microstructure of the sintered ceramics and the templated ceramics exhibited higher values (ε_r~ 48 and τ_f ~ -10 ppm/ ^oC) for the electrical properties when compared to samples prepared without templates (ε_r~ 44 and τ_f ~ -15 ppm/ ^oC). Likewise, the effect of orientation of grains, processing and forming composites on the dielectric losses has been addressed for various oxides [10, 17, 18]. Li et al. [17] used glass as

additive to improve the density of the BLT system and attain τ_f close to zero (- 7 ppm/ ^oC). In the case of other anisotropic compound $BaNd_2Ti_5O_{14}$ (BNT) thick films [10], a textured microstructure results in a temperature dependence of the τ_{ε_r} that could be controllably varied from negative (-114 ppm/^oC) to positive (+12 ppm/^oC) with an increase of the grain aspect ratio as a result of constrained sintering. More recently the microwave properties of $Ba_{0.2}Sr_{0.8}La_4Ti_4O_{15}$ ceramics doped with La_2O_3-B_2O_3-TiO_2 were reported where dielectric properties can be tuned by microstructure [19]. More recently, Boonlakhom et al. [20] demonstrates by engineering the grain boundary for $CaCuTi_4O_{12}$ the losses for the dielectric material can be tuned.

All the above studies reflects the sintering temperature and time were thus considered as significant variables in the control of MW properties with a wide range of ε_r (45 to 70) achievable with near zero τ_{ε_r} and high Qf.

In bulk ceramics used in resonator and antenna applications, there are several strategies available to control the microstructure, which could in the case of BLT lead to enhancement of the MW properties. These include controlling sintering variables such as temperature, time, atmosphere and applying external pressure, electrical or magnetic field. Before more complex external forces are considered, the effect of sintering temperature on the electrical properties of BLT needs to be understood. Therefore, in the present work the evolution of electrical properties of BLT with sintering temperature is systematically investigated and the relations between structure, microstructure and properties established.

II. Experimental

$BaLa_4Ti_4O_{15}$ (1:2:4) (BLT) powders were synthesised by solid state reaction using $BaCO_3$ (Aldrich, Product No.: 513-77-9, purity>99.9%), purity >99.9%), La_2O_3 (Aldrich, purity>99.9%),) and TiO_2 (Aldrich, Product No.:1317-80-2, purity >99.9%) as precursors. Prior to weighing the powders the lanthanum precursor (due to its hydroscopic nature) was heat treated at 800 ºC for 2 h to remove the water and desiccate the precursor in order to avoid absorption of water. Later, the powders were weighed according to the stoichiometry and ball milled in ethanol media, followed by drying at 100 ^oC for 12 h. The dried powders were calcined at temperatures above 1100 ºC to form hexagonal (1:2:4) (BLT). Monophasic BLT calcined powders were re-milled to reduce the particle size. Green pellets of BLT were prepared by uniaxial pressing at 100

MPa followed by isostatically pressing at 200 MPa. The pellets were sintered at temperatures ranging from 1400 to 1600 ^{o}C with heating and cooling rate of 2 ^{o}C/min. The density of BLT ceramics was measured by Archimedes method in diethyl phthalate (Fluke, 8080 with density of 1.118 g/cm^3).

The phase evolution for BLT was carried by X-ray diffraction (XRD, PANalytical X'Pert PRO) on calcined powders at different temperature. The anisotropy of the sintered BLT pellets were investigated by XRD. Also, the anisotropy effect was investigated by RAMAN spectroscopy, using RENISHAW machine equipped with He-Ne laser source with 633 nm wavelength and optical lens of 50x. The error associated with RAMAN measurements is 1 cm^{-1}. Microstructural evolution was followed by scanning electron microscopy (SEM) (Hitachi SU-4100) and grain size calculations were performed using Image J software. The compositional homogeneity of BLT ceramics sintered at different temperature was verify by Energy Dispersive Spectroscopy (EDS) equipped with SEM (FEI Inspect-F Oxford, operated at 20 kV). The relative permittivity (ε_r), loss tangent (tan δ) and temperature coefficient of relative permittivity (τ_{ε_r}) were evaluated in the parallel direction of pressing over a frequency range from 100 kHz to 1 MHz, using an impedance bridge (HP 4284A). The τ_{ε_r} were measured from 30 ^{o}C to 100 ^{o}C. Electrical measurements were carried out using a metal-insulator-metal (MIM) configuration. For that the opposite faces of the ceramic cylinders were polished to ensure parallel surfaces and then gold electrodes were sputtered on them.

III. Results and Discussion

In order to have homogeneous hexagonal BLT oxide, the BLT phase formation and intermediate phase reaction between precursors was studied by XRD between the temperature ranges from 1200 ^{o}C to 1300 ^{o}C for 3 h. The XRD patterns of BLT powders calcined at different temperatures are shown in Fig. 1. At 1200 ^{o}C, the dominant phases are $BaTiO_3$, $La_2Ti_2O_7$ and La_2TiO_5 with a small quantity of hexagonal BLT (ICDD - #01-070-6341). By increasing the calcination temperature, all the phases react to form $BaLa_4Ti_4O_{15}$ at 1300 ^{o}C for 3 h. These results corroborate those reported by Fukami et al. [16] for BLT powders prepared by molten salt synthesis method. The proposed phase formation reaction for BLT synthesised by solid-state reaction is thus:

$La_2O_3 + 2TiO_2 \rightarrow La_2Ti_2O_7$ (1)

$La_2O_3 + TiO_2 \rightarrow La_2TiO_5$ (2)

$BaCO_3 + TiO_2 \rightarrow BaTiO_3 + CO_2$ (3)

$BaTiO_3 + La_2Ti_2O_7 + La_2TiO_5 \rightarrow BaLa_4Ti_4O_{15}$ (4)

BLT ceramics sintered between 1400 and 1600 ^oC present dense microstructures with evidence of anisotropic grain growth. Fig. 2 illustrates the microstructures of ceramics sintered from 1450 to 1600 ºC for different periods of time. The relative density of all the ceramics is around 95 % (Table 1). The aspect ratio of the grains varies from 3 to 24 with increase of sintering temperature from 1400 ºC to 1600 ºC (Table 1). For sintering temperatures up to 1500 ºC the longest grain dimension varies between 5 to 20 µm and it increases drastically with sintering temperature to 52 µm, concomitantly there is a marginal decrease (~1%) in the density of the samples sintered at high temperatures that might be due to abnormal anisotropic grain growth resulting in the entrapment of some pores in the grains. The anisotropy in the microstructure behaviour of BLT (1:1:4) ceramics is clear from the above microstructures and it increases with sintering temperature.

Back scattered electron images revealed that some of the BLT grains have a slightly different contrast, marked in Fig. 3, might indicate a deviation in chemical composition. Chemical elemental mapping was performed and indeed it was observed that some elongated grains were deficient in La as reported by Zheng et al. [6] who related their observations to the presence of two hexagonal phases of slightly different lattice parameter. However, EDS profile carried out on BLT ceramics sintered at different temperature does not shows noticeable changes in the composition of BLT (Fig. 3 (e)) and this observation corroborates elemental mapping and XRD analysis where secondary phases have not been observed.

Fig. 4(a) and (b) reveal the ε_r and dielectric loss of BLT ceramics sintered at different temperatures as a function of frequency and temperature. As sintering temperature increases, ε_r increases until 1500 ºC, reaching a maximum of 51 at 1 MHz frequency but above 1500 ^oC, ε_r decreases (Fig. 4(a)). The high dielectric permittivity for BLT sintered at 1500 ^oC may be due to a higher density (96 %) when compared to

the density (<96 %) of the other BLT ceramics sintered at different temperatures as given in Table 1. Losses were measured at 1 MHz and varied between 0.009 and 0.001. The important observation from an application perspective is that ε_r varies linearly with temperature, as illustrated in Fig. 4(b). The linear variation in ε_r was utilised to calculate τ_{ε_r} which increased from -17 to + 64 ppm/ºC depending on sintering temperature. We propose that the change in permittivity and τ_{ε_r} as a function of sintering correlates directly with the observed microstructural changes, specifically the increase in the proportion of elongated grains that grow normal to the pressing axis. Moreover, the changes in τ_{ε_r} from +ve to –ve and then back to +ve as the sintering temperature increases, represents a singular challenge for controlling properties for commercial applications and has never been reported before in BLT ceramics (summarized in Table 2).

To understand the behaviour of ε_r and τ_{ε_r} with sintering temperature, crystalline orientation and grain size and aspect ratio must be considered. XRD patterns of sintered ceramics (perpendicular to pressed direction) from 1450 to 1600 ºC are depicted in Fig. 5(b). A closer look at these patterns reveals that the ratio between the 00010/11-20 peak drastically changes with sintering temperature from 0.652, at 1450 ºC to 4.469 at 1600 ºC. Thus, it is concluded that at a sintering temperature of 1600 ºC, the grains are considerably more oriented towards the ´c` axis which is reflected in the Fig. 2 average aspect ratio (24) and maximum grain size (52 µm along major axis). According to previous reports, when the intensity ratio 00010/11-20 of BLT is close to 0.5, τ_f (α - τ_{ε_r}) is negative and close to zero.

Further, structural changes were verified by studying the phonon mode using Raman spectroscopy and presented in Fig. 6. BLT is a $Ba_5Nb_4O_{15}$ [21] analogue, a having centrosymmetric hexagonal structure with space group $P\bar{3}c1$ and its point group D3d (-3m). One can expect 72 normal modes of vibration for the tilted BLT compound; for BLT with D3d symmetry the space group predicts the irreducible optic modes:

$$\Gamma optic = 12A1g + 12A1u + 14A2g + 13A2u + 25Eu + 26Eg$$

Among these BLT depicts 38 Raman active modes: 12 A1g + 26 Eg.

To understand the variation in the anisotropy of the BLT ceramics sintered at different temperature Raman spectra were recorded in both perpendicular and parallel

(to the pressing direction) surface of the pellets. The spectra were recorded between 100 cm^{-1} and 1000 cm^{-1} (Fig. 6) and two intense peaks are visible; one below 200 cm^{-1} assigned to stretching of metal – oxygen ions between the perovskite slabs named as La – O (at 130 cm^{-1}) and Ba – O (148 cm^{-1}) and other one at 732 cm^{-1} due to stretching of corner sharing TiO6 octahedra. The vibration peaks between the 200 cm^{-1} and 900 cm^{-1} are due to symmetric and asymmetric bending and stretching vibration of the TiO6 octahedra.

The Raman spectra recorded from BLT sintered at different temperature does not show any significant changes in peak position, but instead reveals an intensity variation of the vibration peaks at 130 cm^{-1} and 148 cm^{-1} assigned to A – O ions bonds (where A is Ba, and La) and of the octahedra asymmetric doublet bending peaks at 276 cm^{-1} and 294 cm^{-1}. For samples sintered at 1450 ^{o}C and 1500 ^{o}C, the Raman spectra from parallel and normal direction to the pressing surface does not show any significant changes in the intensity of the peaks assigned to A – O ion bonding (at 130 cm^{-1} and 148 cm^{-1}) nor TiO_6 octahedra asymmetric doublet peaks (at 274 and 294 cm^{-1}). Clearly suggesting no signs of changes at the level of A – O ions bonding and consequently of TiO6 asymmetry bending modes in BLT ceramics sintered at 1450 ^{o}C and 1500 ^{o}C. Whereas for BLT ceramics sintered at 1550 ^{o}C and 1600 ^{o}C, the Raman spectra from parallel and normal direction to the surface to pressing presents significant changes in the intensity of 130 cm^{-1} and 148 cm^{-1} and 276 cm^{-1} and 294 cm^{-1} peaks. The change in the intensity of the A – O vibration mode affects the lattice environment resulting in the change in the intensity of asymmetric bending and stretching vibration TiO_6 octahedra modes. These variations are associated with the orientation of the crystal and can be related with XRD observations of a ´c` axis preferential oriented ceramics and also with the dielectric properties [22].

In the present studies we found there is a small window where τ_{ε_r} changes sign from positive to negative for BLT sintered at 1500 ºC at which temperature the intensity ratio of 00010/11-20 peaks is 0.819 with a grain aspect ratio 15-20.

A similar change in sign of the temperature coefficient of capacitance (τ_C) has been reported for $La_2Ti_2O_7$ fabricated by hot-forging for which τ_C = +188 ppm/ºC and -14 ppm/ºC and ε_r = 42.5 and 54.1 when measured parallel to the 010 axis (b direction) and 010 direction (along a and c direction), respectively. Randomly oriented samples prepared by conventional sintering exhibit intermediate values [23]. The large ε_r and

change in the sign of τ_C for oriented $La_2Ti_2O_7$ clearly supports our observations for the BLT. Furthermore, Fukami et al. [16] produced BLT ceramics using BLT templates and reported that τ_f approached zero (-16 to -10 ppm/ºC) and ε_r increased up to a template concentration of 30 % (from 45 to 48). With further increase in the template concentration to 50 % there is a decrease in ε_r (~ 46) and τ_f becomes positive (+ 6 ppm/ºC). The authors state that the changes in properties are due to the formation of a secondary phase ($La_2Ti_2O_7$). However, by comparing the grain size of the SEM micrograph for the template BLT ceramics produced from 50 % template concentration, with that obtained in this work for BLT sintered at 1500 ºC, both microstructures are similar and we postulate that the changes on properties observed by Fukami et al. [16] with sintering may well relate to changes in grain orientation and aspect ratio.

A double zero crossing for the variation of τ_{ε_r} with the sintering temperature was also reported by Bendersky et al. [24] for $Ca_5Nb_2TiO_{12}$ and $Ca_5Ta_2TiO_{12}$ systems. In this study, the authors suggested that the variation in τ_{ε_r} related to ordering of cations on the B sites, but HRTEM studies were inconclusive. Grain structures of $Ca_5Nb_2TiO_{12}$ and $Ca_5Ta_2TiO_{12}$ are similar to that of BLT and an alternative explanation is that there are similar microstructural / orientation changes to those described in this study.

IV. Conclusions

BLT ceramics possess microstructures in which anisotropic grain growth takes place with increasing sintering temperature, which results in a non-monotonous increase in ε_r. At 1500 ºC, ε_r reaches a maximum of 51, with tan δ minimum at 0.002 and τ_{ε_r} = -17 ppm/ºC at 1 MHz. Since ε_r and $\tau_{\varepsilon_r}$are directly proportional in the absence of a phase transition [15], the variation of τ_{ε_r} as a function of the sintering temperature is also nonlinear, showing a double crossover of τ_{ε_r}. This behaviour is related with variations in the orientation (ratio of 00010/11-20 peak of the BLT hexagonal structure) and aspect ratio and size distribution of the grains with sintering temperature. The combination of an elongated anisotropic grain microstructure with a preferential crystallographic orientation gives an optimised τ_{ε_r} and it is demonstrated that by controlling sintering conditions, microwave dielectric properties can be tuned without the need for templating. It is proposed that this is a general phenomenon which can also

be used to explain the variation in, and tune the properties of, other ceramic systems with anisotropic grain structures such as $La_2Ti_2O_7$ [23] and $Ca_5(Ta,Nb)_2TiO_{12}$ [24].

Acknowledgments

The authors acknowledge Fundação para a Ciência e a Tecnologia (FCT), Fundo Europeu de Desenvolvimento Regional Portugal (FEDER), QREN-COMPETE Portugal, and the Associate Laboratory CICECO (PEst-C/CTM/LA0011/2013) for funding support. Amit Mahajan acknowledges FCT for financial support (SFRH / BD / 65415 / 2009).

References

[1] H. Zheng, I.M. Reaney, D. Muir, T. Price, D.M. Iddles, Effect of glass additions on the sintering and microwave properties of composite dielectric ceramics based on BaO–Ln_2O_3–TiO_2 (Ln = Nd, La), Journal of the European Ceramic Society 27(16) (2007) 4479-4487.

[2] H.M. O'Bryan, J. Thomson, J.K. Plourde, A new BaO-TiO_2 compound with temperature-stable high permittivity and low microwave loss, J. Am. Ceram. Soc. 57(10) (1974) 450-453.

[3] K. Wakino, K. Minai, H. Tamura, Microwave characteristics of (Zr, Sn)TiO_4 and BaO-PbO-Nd_2O_3-TiO_2 dielectric resonators, J. Am. Ceram. Soc. 67(4) (1984) 278-281.

[4] U. Ullah, W.F.F.W. Ali, M.F. Ain, N.M. Mahyuddin, Z.A. Ahmad, Design of a novel dielectric resonator antenna using $MgTiO_3$–$CoTiO_3$ for wideband applications, Materials & Design 85 (2015) 396-403.

[5] X. Chou, Z. Zhao, W. Zhang, J. Zhai, Microstructures and dielectric properties of $Ba_{0.5}Sr_{0.5}TiO_3$–Zn_2TiO_4 composite ceramics with low sintering temperature for tunable device applications, Materials & Design 31(8) (2010) 3703-3707.

[6] H. Zheng, D.I. Woodward, L. Gillie, I.M. Reaney, Structure and microwave dielectric properties of $BaLa_4$ Ti_4O_{15}, Journal of Physics: Condensed Matter 18(31) (2006) 7051.

[7] N.I.S. Isuhak Naseemabeevi Jawahara, Mailadil Thomas Sebastiana and Pezholil Mohanana Microwave dielectric properties of MO-La_2O_3-TiO_2 (M = Ca, Sr, Ba) ceramics, J. Mater. Res. 17 (2002) 3084-3089

[8] H. Ohsato, Y. Tohdo, K. Kakimoto, T. Okawa, H. Okabe, Crystal structure and microwave dielectric properties of $Ba_nLa_4Ti_{3+n}O_{12+3n}$ homologous compounds with high dielectric constant and high quality factor, 27th Annual Cocoa Beach Conference on Advanced Ceramics and Composites-B: Ceramic Engineering and Science Proceedings, John Wiley & Sons, 2009, pp. 75-80.

[9] O. Takashi, K. Katsumasa, O. Hiroki, O. Hitoshi, Microwave dielectric properties of $Ba_nLa_4Ti_{3+n}O_{12+3n}$ homologous series, Jpn. J. Appl. Phys. 40(9S) (2001) 5779.

[10] Z. Fu, P.M. Vilarinho, A. Wu, A.I. Kingon, Textured microstructure and dielectric properties relationship of $BaNd_2Ti_5O_{14}$ thick films prepared by electrophoretic deposition, Advanced Functional Materials 19(7) (2009) 1071-1081.

[11] B.-J. Li, S.-Y. Wang, Y.-h. Liao, S.-H. Lin, Y.-B. Chen, High dielectric constant and low loss microwave dielectric ceramics of $(1-y)(Mg_{0.95}\ Co_{0.05})_2\ (Ti_{0.95}\ Sn_{0.05})O_4$–y $(Ca_{0.61}\ Nd_{\ 0.8/3})\ TiO_3$ for microwave applications, Journal of the Ceramic Society of Japan 124(4) (2016) 460-463.

[12] P.M. Vilarinho, A. Mahajan, I. Sterianou, I.M. Reaney, Layered composite thick films for dielectric applications, Journal of the European Ceramic Society 32(16) (2012) 4319-4326.

[13] G. Trolliard, N. Harre, D. Mercurio, B. Frit, Cation-deficient perovskite-related $(Ba,La)_nTi_{n-\delta}O_{3n}$ ($n \geq 4\delta$) microphases in the $La_4Ti_3O_{12}$–$BaTiO_3$ system: an HRTEM approach, Journal of Solid State Chemistry 145(2) (1999) 678-693.

[14] N. Harre, D. Mercurio, G. Trolliard, B. Frit, Crystal structure of $BaLa_4Ti_4O_{15}$, member n = 5 of the homologous series $(Ba,\ La)_nTi_{n-1}O_{3n}$ of cation-deficient perovskite-related compounds, Mater. Res. Bull. 33(10) (1998) 1537-1548.

[15] N. Teneze, D. Mercurio, G. Trolliard, B. Frit, Cation-deficient perovskite-related compounds (Ba,La)nTin–1O3n (n = 4, 5, and 6): a rietveld refinement from neutron powder diffraction data, Mater. Res. Bull. 35(10) (2000) 1603-1614.

[16] Y. Fukami, K. Wada, K. Kakimoto, H. Ohsato, Microstructure and microwave dielectric properties of $BaLa_4Ti_4O_{15}$ ceramics with template particles, Journal of the European Ceramic Society 26(10–11) (2006) 2055-2058.

[17] Y.-x. Li, F. Si, B. Tang, Y. Wang, S.-r. Zhang, Microwave Dielectric Properties of $Ba_{0.2}Sr_{0.8}La_4Ti_4O_{15}$ Ceramic with La_2O_3-B_2O_3-TiO_2 Doping, Journal of Electronic Materials 45(2) (2016) 1011-1016.

[18] J. Bi, Y. Gu, Z. Zhang, S. Wang, M. Li, Z. Zhang, Core–shell SiC/SiO_2 whisker reinforced polymer composite with high dielectric permittivity and low dielectric loss, Materials & Design 89 (2016) 933-940.

[19] Q. Xu, X.-F. Zhang, H.-X. Liu, W. Chen, M. Chen, B.-H. Kim, Effect of sintering temperature on dielectric properties of $Ba_{0.6}Sr_{0.4}TiO_3$–MgO composite ceramics prepared from fine constituent powders, Materials & Design 32(3) (2011) 1200-1204.

[20] J. Boonlakhorn, B. Putasaeng, P. Kidkhunthod, P. Thongbai, Improved dielectric properties of (Y + Mg) co-doped $CaCu_3Ti_4O_{12}$ ceramics by controlling geometric and intrinsic properties of grain boundaries, Materials & Design 92 (2016) 494-498.

[21] R. Ratheesh, H. Sreemoolanadhan, M.T. Sebastian, Vibrational analysis of $Ba_{5-x}Sr_xNb_4O_{15}$ microwave dielectric ceramic resonators, Journal of Solid State Chemistry 131(1) (1997) 2-8.

[22] N.E. Massa, S. Pagola, R. Carbonio, Far-infrared reflectivity and Raman spectra of $Ba_5Nb_4O_{15}$, Physical Review B 53(13) (1996) 8148-8150.

[23] P.A. Fuierer, R.E. Newnham, $La_2Ti_2O_7$ Ceramics, J. Am. Ceram. Soc. 74(11) (1991) 2876-2881.

[24] L.A. Bendersky, J.J. Krajewski, R.J. Cava, Dielectric properties and microstructure of $Ca_5Nb_2TiO_{12}$ and $Ca_5Ta_2TiO_{12}$, Journal of the European Ceramic Society 21(15) (2001) 2653-2658.

Fig. Captions:

Fig. 1: XRD patterns of BLT calcined at different temperatures. Intermediate phases as $BaTiO_3$, $La_2Ti_2O_7$ and La_2TiO_5 dominate these patterns at temperatures below 1300 ºC. A monophasic hexagonal (1:2:4) BLT is obtained at 1300 ºC.

Fig. 2: SEM micrographs of BLT ceramics sintered at different temperatures: a) 1450 ºC, b) 1500 ºC, c) 1550 ºC and d) 1600 ºC. As the sintering temperature increases the grain size increases along with the aspect ratio (Table I).

Fig. 3: SEM micrographs of BLT ceramics sintered at 1550 ºC (a). Elemental mapping of (b) Lanthanum and (c) Barium. Back scattered micrograph of 1450 ºC with lanthanum deficient phase encircled in red (d). Elemental mapping and back scattered SEM suggest that some of the elongated grains are deficient in lanthanum. EDS profile from BLT ceramics sintered at different temperatures (scan area 40 um X 40 um) (e) does not show overall changes in the composition.

Fig. 4: Dielectric properties of BLT ceramics sintered at different temperatures: a) relative permittivity and losses as a function of frequency (up to 1 MHz) and b) relative permittivity as a function of temperature, measured at 1 MHz from temperature ranges from 30 to 100 ºC.

Fig. 5: (a) τ_{ε_r} and relative permittivity as a function of sintering temperature for BLT ceramics at 1 MHz and (b) XRD spectra from 2θ = 30 to 45 ^{o} for BLT ceramics sintered at 1450 ^{o}C, 1500 ^{o}C, 1550 ^{o}C and 1600 ^{o}C, depicts the intensity ratio between 00010 plane and 11-20 plane.

Fig. 6: Raman spectra from the surface of BLT ceramics perpendicular and parallel (marked as C/S, cross section) to the pressing direction, sintered at 1450 ^{o}C, 1500 ^{o}C, 1550 ^{o}C and 1600 ^{o}C. The variation in peak intensity at 130 cm^{-1} and 148 cm^{-1} assigned to A – O bonds vibrations and 276 cm^{-1} and 294 cm^{-1} assigned to asymmetric bending and stretching vibration of the TiO6 octahedra for BLT sintered at 1550 ^{o}C and 1600 ^{o}C points to the crystalographic anisotropy of BLT ceramics sintered at high temperatures.

Table 1: Physical parameters of hexagonal (1:2:4) BLT ceramics sintered at different temperatures.

Table 2: Dielectric characteristics of BLT ceramics.

Figures :

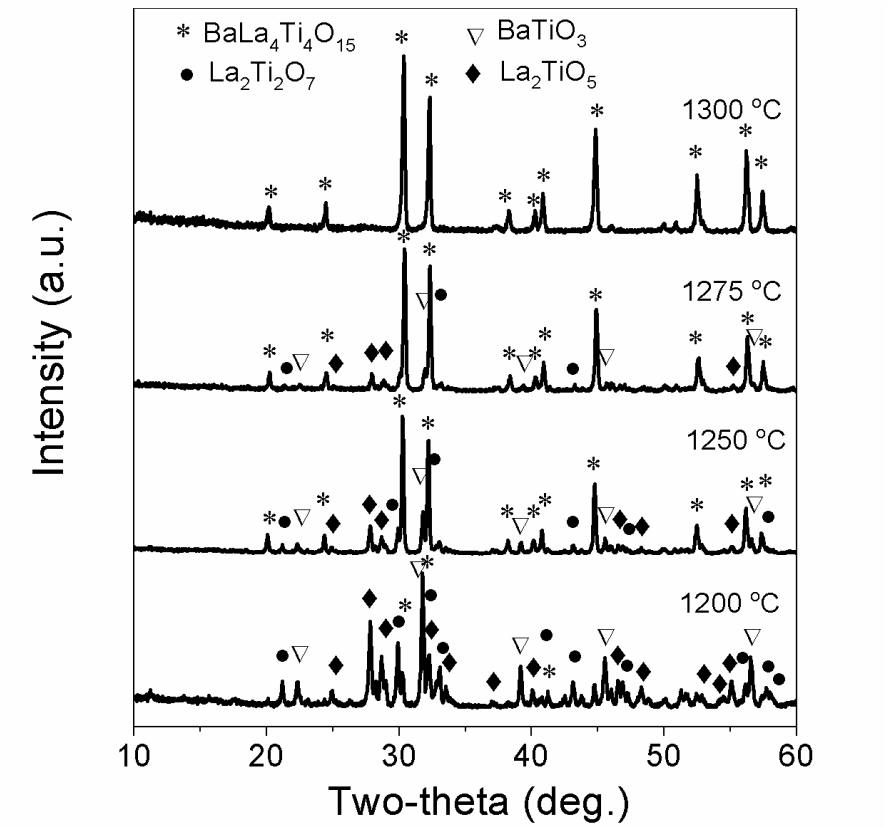

Fig. 1: XRD patterns of BLT calcined at different temperatures. Intermediate phases as $BaTiO_3$, $La_2Ti_2O_7$ and La_2TiO_5 dominate these patterns at temperatures below 1300 ºC. A monophasic hexagonal (1:2:4) BLT is obtained at 1300 ºC.

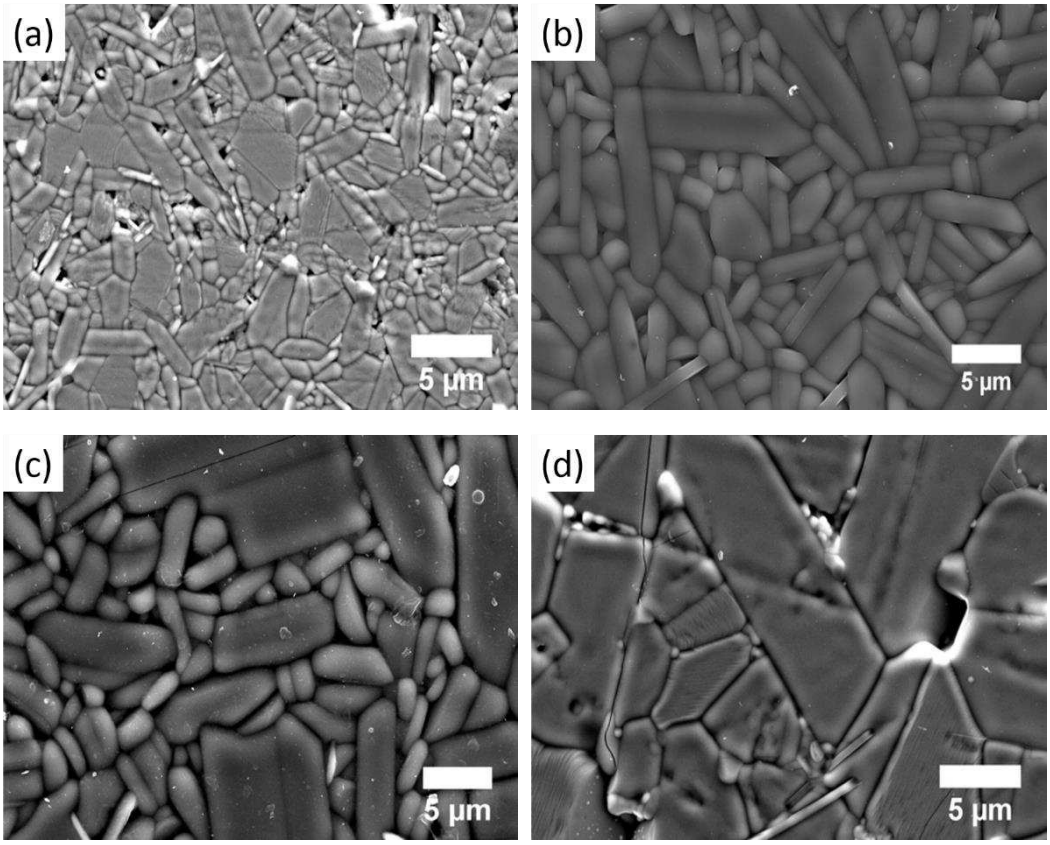

Fig. 2: SEM micrographs of BLT ceramics sintered at different temperatures: a) 1450 ºC, b) 1500 ºC, c) 1550 ºC and d) 1600 ºC. As the sintering temperature increases the grain size increases along with the aspect ratio (Table I).

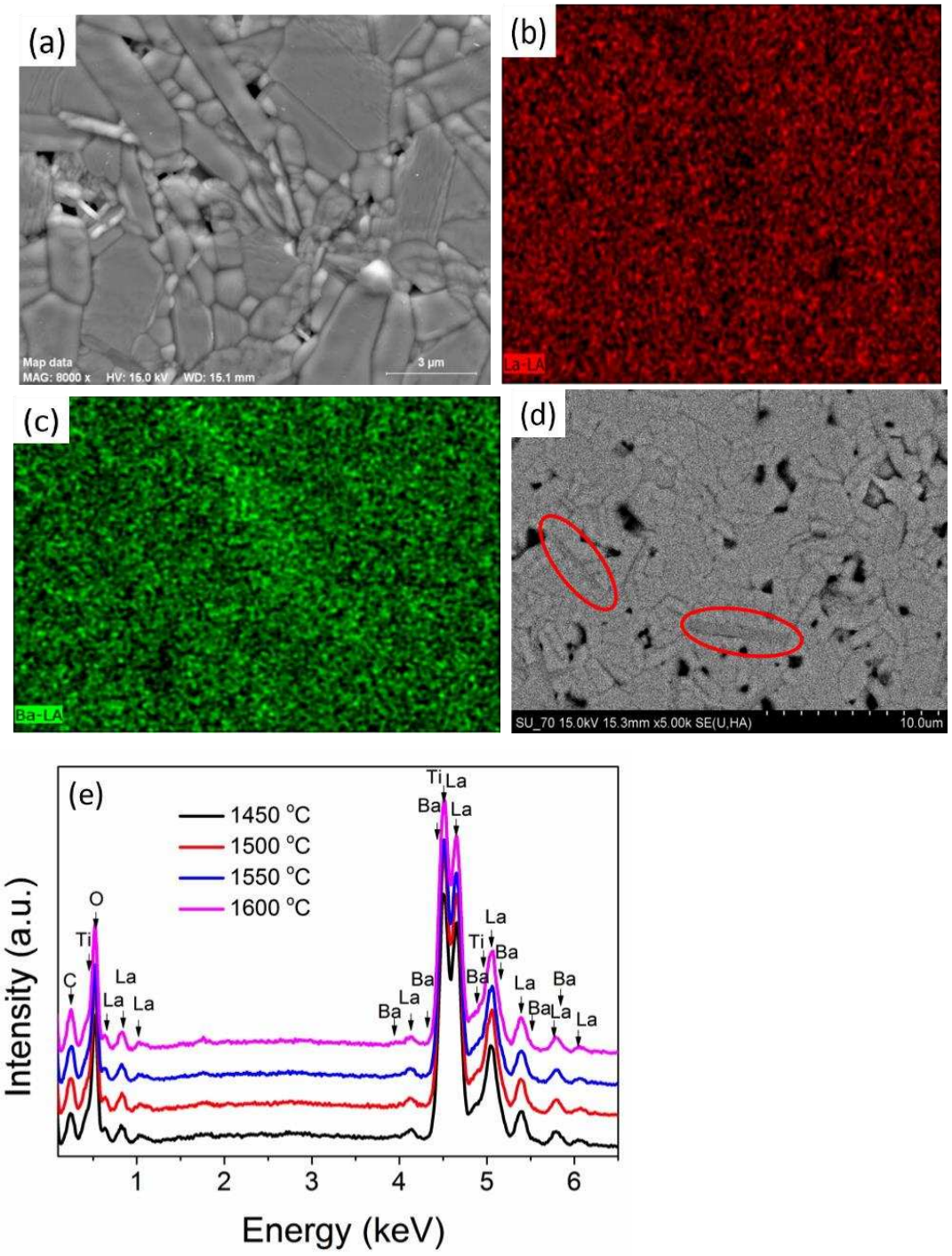

Fig. 3: SEM micrographs of BLT ceramics sintered at 1550 ºC (a). Elemental mapping of (b) Lanthanum and (c) Barium. Back scattered micrograph of 1450 ºC with lanthanum deficient phase encircled in red (d). Elemental mapping and back scattered SEM suggest that some of the elongated grains are deficient in lanthanum. EDS profile

from BLT ceramics sintered at different temperatures (scan area 40 um X 40 um) (e) does not show overall changes in the composition.

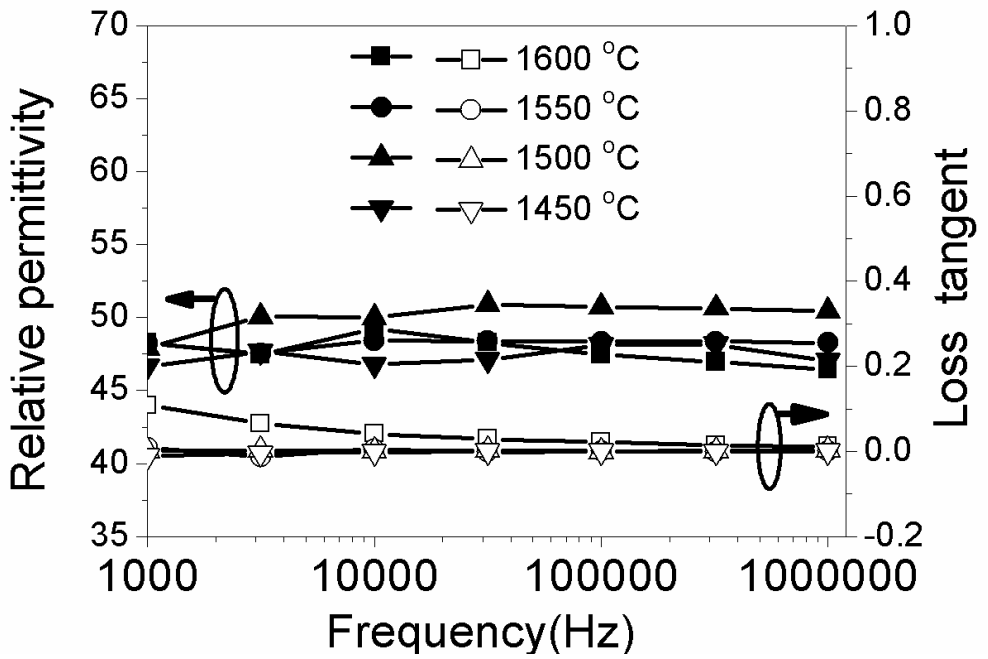

(a)

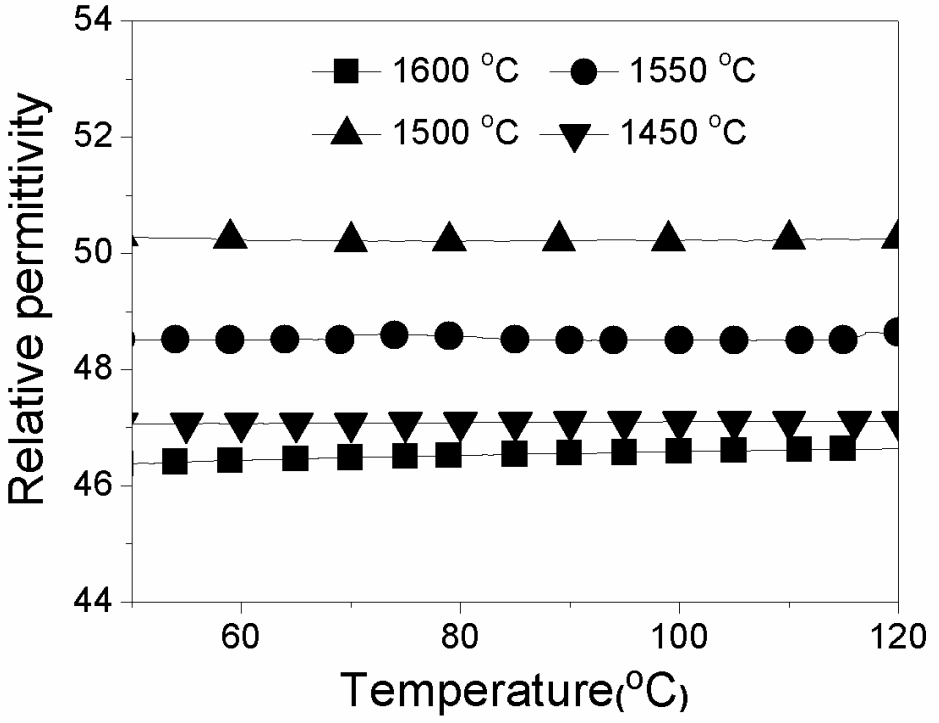

(b)

Fig. 4: Dielectric properties of BLT ceramics sintered at different temperatures: a) relative permittivity and losses as a function of frequency (up to 1 MHz) and b) relative permittivity as a function of temperature, measured at 1 MHz from temperature ranges from 30 to 100 ºC.

.

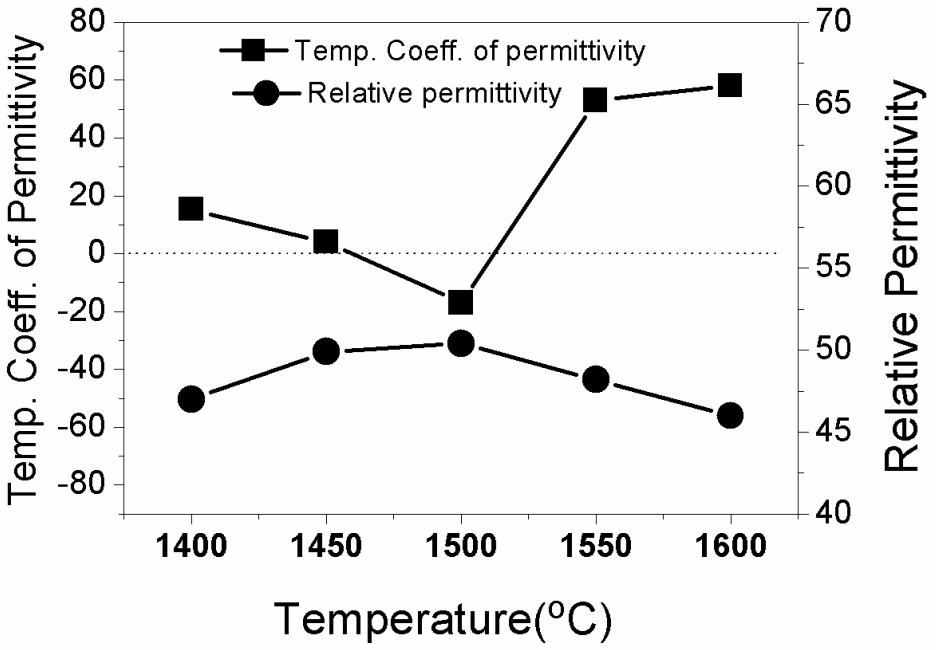

(a)

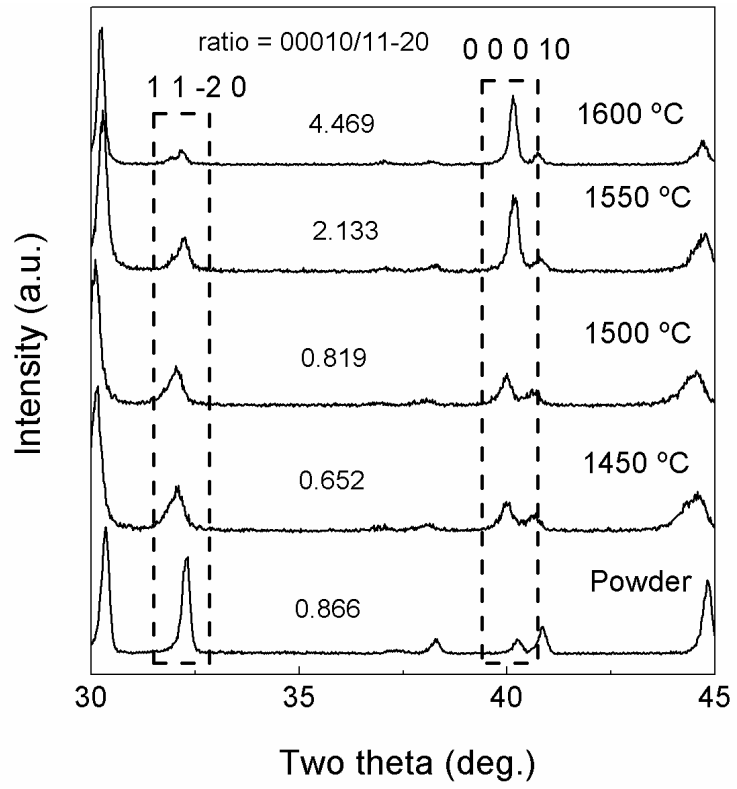

(b)

Fig. 5: (a) τ_{ε_r} and relative permittivity as a function of sintering temperature for BLT ceramics at 1 MHz and (b) XRD spectra from 2θ = 30 to 45 ^{o} for BLT ceramics sintered at 1450 ^{o}C, 1500 ^{o}C, 1550 ^{o}C and 1600 ^{o}C, depicts the intensity ratio between 00010 plane and 11-20 plane.

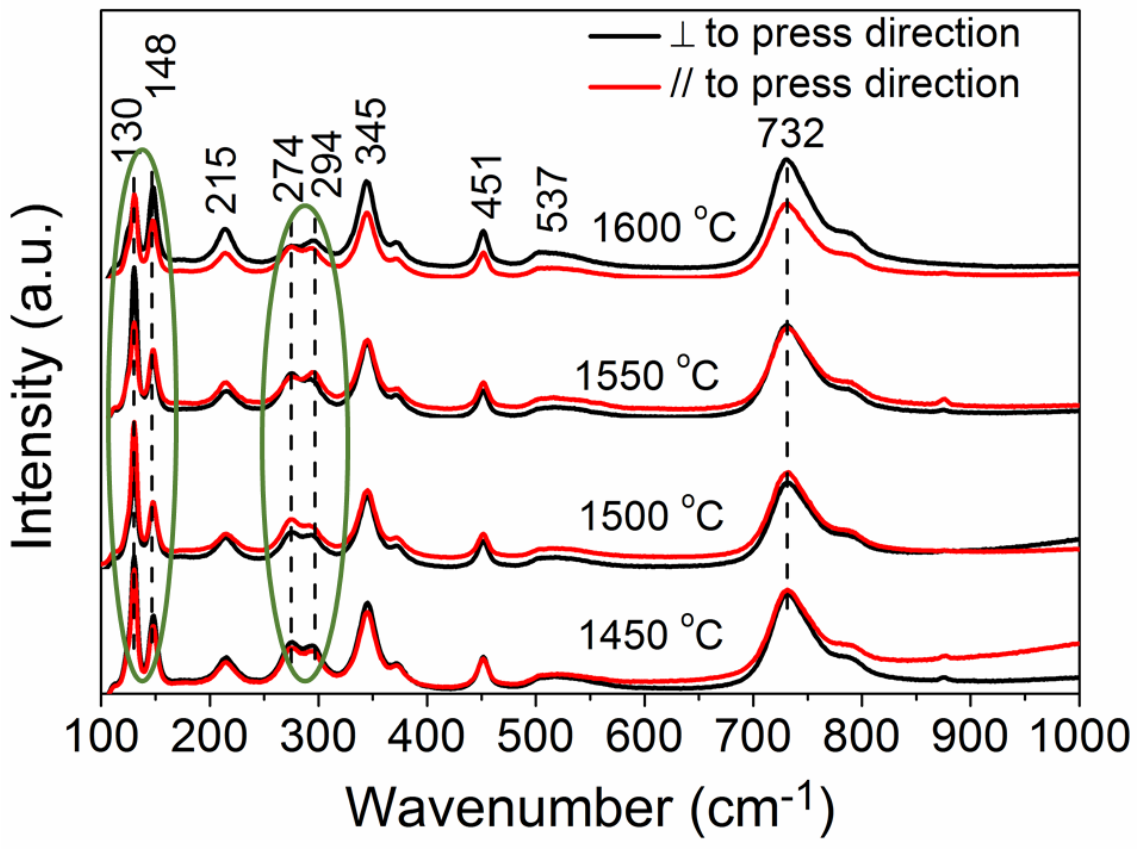

Fig. 6: Raman spectra from the surface of BLT ceramics perpendicular and parallel (marked as C/S, cross section) to the pressing direction, sintered at 1450 ^{o}C, 1500 ^{o}C, 1550 ^{o}C and 1600 ^{o}C. The variation in peak intensity at 130 cm^{-1} and 148 cm^{-1} assigned to A – O bonds vibrations and 276 cm^{-1} and 294 cm^{-1} assigned to asymmetric bending and stretching vibration of the TiO6 octahedra for BLT sintered at 1550 ^{o}C and 1600 ^{o}C points to the crystalographic anisotropy of BLT ceramics sintered at high temperatures.

Tables

Table 1: Physical parameters of hexagonal (1:2:4) BLT ceramics sintered at different temperatures.

Sintering temperature (^{o}C)	**Relative density**	**Average maximum aspect ratio of the grain**	**Average maximum size of the grain in longer axis (μm)**
1400	93%	3	5
1450	94%	5	6
1500	96%	10	15 -20
1550	95%	22	52
1600	95%	24	52

Table 2: Dielectric characteristics of BLT ceramics.

Sintering temperature (°C)	**Permittivity at 1MHz**	**Loss tangent at 1MHz**	τ_{ε_r} **(30-100)°C (ppm/°C)**
1450	44	0.001	+4
1500	51	0.002	-17
1550	48	0.002	+44
1600	46	0.001	+62